Contents lists available at ScienceDirect

Digital Chinese Medicine

journal homepage: http://www.keaipublishing.com/dcmed

Perturbations in gastrointestinal tract microbiota composition and function in individuals with yellow-greasy tongue coating

LIU Zhanyan[a, b†], LI Zhiyue[b†], ZHU Guanbao[b, c], LIU Yaqian[b], PENG Qinghua[a*], WU Zhengzhi[b, d*]

a. School of Traditional Chinese Medicine, Hunan University of Chinese Medicine, Changsha, Hunan 410208, China

b. Shenzhen Institute of Geriatrics, The First Affiliated Hospital of Shenzhen University, Shenzhen, Guangdong 518035, China

c. Graduate School, Guangxi University of Chinese Medicine, Nanning, Guangxi 530200, China

d. WU Zhengzhi Academician Workstation, Ningbo College of Health Sciences, Ningbo, Zhejiang 315800, China

ARTICLE INFO

Article history
Received 22 March 2023
Accepted 26 May 2023
Available online 25 June 2023

Keywords
Gut microbiota
Yellow-greasy tongue coating
Microcosmic syndrome differentiation
16S rRNA
Metagenome
Metabonomics

ABSTRACT

Objective To study the composition and function of tongue coating (TC) and gastrointestinal tract (GIT) microbiota in participants with yellow-greasy tongue coating (YGTC), and to explore the representative metabolite markers and pathways in this group.

Methods Subjects with YGTC or thin-white tongue coating (TWTC) were recruited from December 1, 2021 to October 30, 2022, and the TC and fecal samples were collected. Samples were subjected to both whole-genome shotgun (WGS), and 16S rRNA gene sequencing. The α-diversity analysis, principal component analysis (PCA), and Spearman correlation analysis were performed for two groups. Ultra-performance liquid chromatography combined with tandem mass spectrometry (UPLC–MS/MS) analysis was used to analyze metabolomics and enrichment of metabolic pathways.

Results The results revealed 20 YGTC participates and 19 TWTC participates. At the genus level, the dominant bacterial species of TC flora and intestinal flora in the two groups were roughly the same, but the relative kurtosis difference was marked, and the abundance of potentially pathogenic bacteria in TC and fecal samples of YGTC subjects was higher. There were 9 down-regulated microorganisms in the TC samples, 26 down-regulated microorganisms, and 6 up-regulated microorganisms in YGTC subjects. The α-diversity analysis indicated that the Chao and abundance-based coverage estimator (ACE) indices of TC bacteria in the YGTC subjects showed a decreasing trend, but the difference was not statistically significant ($P > 0.05$). The α-diversity of fecal samples and the Chao and ACE indices decreased significantly ($P < 0.05$). PCA showed that the microflora structure of TC and fecal samples were significantly different between the two groups. Spearman correlation analysis showed that there was no correlation between TC and fecal microorganisms at phyla and genus levels in the same subjects ($P > 0.05$). The metabolomics results demonstrated that fumarate reductase, V/A ATPase, and phosphatidylethanolamine were increased, and glycerate-3p, UDP-glucose, and quinone oxidoreductase metabolites were decreased in YGTC TC samples. Inosine monophosphate (IMP), uridine monophosphate (UMP), and gamma-aminobutyric acid (GABA) were increased in YGTC fecal samples, while the contents of ribo-5P, histidine, biotin,

†The authors contributed equally.

*Corresponding author: WU Zhengzhi, E-mail: szwzz001@163.com. PENG Qinghua, E-mail: pqh410007@126.com.

Peer review under the responsibility of Hunan University of Chinese Medicine.

DOI: 10.1016/j.dcmed.2023.07.006

Citation: LIU ZY, LI ZY, ZHU GB, et al. Perturbations in gastrointestinal tract microbiota composition and function in individuals with yellow-greasy tongue coating. Digital Chinese Medicine, 2023, 6(2): 160-169.

and cobalamin were decreased. Metabolic pathway analysis indicated that the abundance of the TC and fecal samples of the YGTC subjects was relatively low in various metabolic pathways, including amino acid metabolism, carbohydrate metabolism, nitrogen metabolism, and energy metabolism.

Conclusion Structural and functional changes in TC and GIT microbiota or metabolite markers could be potential biological bases of YGTC formation.

1 Introduction

Tongue coating (TC) is mainly composed of exfoliated epithelial cells, bacteria, molds, saliva, and food residues dominated by fungiform papillae and filiform papillae [1]. TC can reflect the health status of the human body. In Chinese medicine, the TC is produced by stomach Qi (Qi of the spleen and stomach) through fumigation, reflecting the functional state of the digestive, endocrine, metabolism, and immune systems with the spleen and stomach as the core [2]. As the vital component of observation diagnosis, tongue diagnosis is one of the main bases for traditional Chinese medicine (TCM) physicians to treat patients based on pattern/syndrome differentiation. Different TCs show different specific microbiota patterns, corresponding to the physiological and pathological changes inside the body. According to the coating quality such as the color, thickness, and wetness, the phenotype of TC can be divided into dozens of categories, such as thin-white coating, yellow-greasy coating, rootless coating, rooted coating, moist coating, and dry coating. The TC of healthy individuals is thin, white, and moist, which is called a thin-white coating. Yellow-greasy coating refers in particular to the yellow and sticky coating on the tongue, which is a common coating for patients with damp-heat patterns in TCM; however, the damp-heat pattern is generally considered to be related to metabolic dysfunction [3]. It was reported that the dominant bacterial groups in white coating and yellow coating were different, which were *Hemolytic streptococcus* and *Catarrh cus*, respectively [4]. In addition, the number of bacteria in the thick coating was bigger than that in the thin coating, and anaerobic bacteria increased and aerobic bacteria decreased in the thick coating [4].

In the physiological state, the flora in the TC stimulates the host immune system, which is conducive to the health of the host, in turn, the host provides a suitable environment and nutrition for microorganisms, and there is a dynamic balance between them. In abnormal conditions, the host's nutritional intake, immunity, diseases, and drug administration will lead to pathological TC, which causes unbalanced macroecology of TC. HSU et al. [5] suggested that the coverage area of yellow-greasy coating, as a typical tongue feature, could be used directly to distinguish type 2 diabetic patients from healthy individuals. HU et al. [6] showed that the TC of patients with gastric cancer was significantly thicker than that of healthy controls, and the species composition of TC was significantly different from that of healthy people. For example, the relative abundance of *Fusobacterium*, *Neisseria*, *Haemophilus,* and *Porphyromonas* on the TC of patients with gastric cancer was lower. ZHAO et al. [7] showed that chronic hepatitis B (CHB) patients with yellow TC had higher viral titers and a significantly lower level of *Bacteroidetes* and a higher level of *Proteobacteria* than the CHB patients with white TC, and macrogenomic sequencing indicated that the metabolic pathway on yellow TC was mainly enriched in amino acid metabolism, which was consistent with the metabolic disorder in the body. The changes in microbiota and microbial metabolites on the TC are closely related to the internal environment. Therefore, the TC serves as an important indicator to reflect the physiological and clinicopathological changes in the inner parts of the body.

However, the present research is limited to the known biological function indexes of the tongue itself to study the principle of TC formation. Based on the interaction between microorganisms and the host immune system, some scholars have proposed that there may be a correlation between intestinal flora and oral flora. Based on TCM theory, the tongue is an outer extension of Pi (spleen-pancreas) and Wei (stomach), TC is condensed stomach Qi and the essence Qi of food, and tongue appearance is a highly sensitive index of the physiological and pathological status of the organs, especially the stomach and spleen. Therefore, we propose a scientific hypothesis that there may be interaction and regular changes between the tongue-gut-microbiota axis, which means that some specific gastrointestinal tract (GIT) microbiota may have a corresponding relationship with the yellow-greasy coating. The relationship between TC and GIT microbiota is one of the most important scientific problems to investigate the internal environment network, which is helpful to reveal the biological basis of TC formation from the level of the overall internal environment. Therefore, from the perspective of the microecological network, this study selected intestinal flora as the starting point, and compared the differences in TC and GIT microecology between individuals with yellow-greasy tongue coating (YGTC) or thin-white tongue coating (TWTC), to find out the special changes of GIT microecology in YGTC, explore the correlation among tongue-gut-microbiota axis,

and provide clinical-basic experimental support for finding GIT microecological changes and preventing chronic diseases by observing YGTC.

2 Methods

2.1 Ethical statement

The experimental protocol was established according to the guidelines of the Declaration of Helsinki, and was approved by the Ethics Committee of the First Affiliated Hospital of Shenzhen University (KS-20190418003). The research has been registered in the China Clinical Trial Center (CHiCTR1900024462).

2.2 Subjects

Participants were recruited at the inpatient service of the Department of Traditional Chinese Medicine of The First Affiliated Hospital of Shenzhen University from December 1, 2021 to October 30, 2022. The subjects were assigned to two groups in accordance with their TCs, including YGTC and TWTC subjects.

2.3 TC classification

We formulated the tongue states table based on the contents of tongue diagnosis according to *Diagnostics of Tradition Chinese Medicine* [8]. The tongue pictures of all subjects were observed and recorded by two qualified and experienced TCM doctors, and then photographed by professional tongue imagers and input into the computer. The diagnostic information of TC was independently determined by three experts to ensure objective evaluation. If the three experts agreed, the subjects would be included in the study. Otherwise, he/she will be excluded.

2.3.1 Diagnostic criteria According to the TC classification standard in *Diagnostics of Traditional Chinese Medicine* [8]: (i) YGTC: the color of the coating is yellow and sticky, coating granules are tight and sticky as yellow powder coating tongue; (ii) TWTC: TC is in a thin white uniform, not sticky or greasy, and not easy to wipe.

2.3.2 Inclusion criteria (i) Adults met the standard of tongue image classification in TCM and followed the specimen collection method specified in this subject; (ii) participants had signed the informed consent.

2.3.3 Exclusion criteria (i) Subjects diagnosed with oral diseases, such as dental caries and periodontal disease; (ii) gargling before sample collection or dental cleaning and extraction within one month; (iii) drug or food dye moss, long-term smoking, scraping moss, and other factors seriously affect the TC; (iv) the use of antibiotics, probiotics, prebiotics, or synbiotics during the previous month; (v) women under pregnancy or lactation.

2.4 TC samples

All subjects were asked to gargle with normal saline before sampling to flush the food contamination that may affect the TC, which has been informed by the subjects. The TC was scraped with a small spoon and the sample was put into a sterilized eppendorff tube containing 2 mL of normal saline. TC samples were stored at room temperature for 1 - 2 h at most and then centrifuged at 2 000× g at 4 °C for 10 min. The supernatant was collected and stored at – 80 °C.

2.5 Fecal sample collection

Each participant was required to use a sterile collection container to collect fresh fecal samples, then placed the container in an icebox and transferred to the laboratory within 2 h, which is packaged into 2 mL cryopreservation tubes and frozen at – 80 °C until RNA extraction.

2.6 RNA extraction for microbiome analysis

Total bacterial RNA was extracted from fecal and TC samples using the TIANamp Bacteria RNA kit (Tiangen, China) according to the manufacturer's protocol.

2.7 16S rRNA gene V3-V4 region sequencing

RNA extracted from each sample was used as a template, and the V3-V4 hypervariable region of the 16S rRNA gene was amplified using polymerase chain reaction (PCR). PCR amplification, sequencing of the PCR amplicons, and quality control of raw data were performed. The raw sequencing data from fecal and TC samples from individual donors were processed into operational taxonomic units at 97% similarity. The α-diversity value was calculated by Mothur (v1.31.2), and the dilution curve was drawn by R language (v3.1.1). Wilcoxon Rank-Sum Test (Wilcox. Test in R language) was used to test the difference between groups.

2.8 Whole-genome shotgun (WGS) sequencing

16S rRNA gene sequencing allows for the taxonomic classification of microbes, and whole metagenome shotgun sequencing enables the identification of potential metabolic functions of microbiota. Fecal and TC samples were used for WMS using the Illumina HiSeq. 4000 platform, with 150-bp paired-end, reads (2 ×150), across 4 lanes. Quality filtering was performed by removing host-contaminated sequences using Bowtie2 (v2.2.5) and applying a conservative quality threshold criterion of

Phred score > 20 and minimum sequence length > 105 bp, using SOAPnuke (v1.5.0). Following quality filtering, filtered reads were processed using the microbial functional profiling tool, Diamond (v2.0.11).

2.9 Ultra-performance liquid chromatography coupled to tandem mass spectrometry (UPLC–MS/MS) analysis

A 5 μL aliquot of the pretreated sample was injected into a 100 mm × 2.1 mm, 1.7 μmol BEH C18 column on a UPLC–MS/MS station. The column temperature was set at 40 °C, and the flow rate was 0.40 mL/min. The mobile phase consisted of two solutions, A (water with 0.1% formic acid) and B (acetonitrile), which were eluted. All analyses were acquired with a locking spray to ensure accuracy and reproducibility.

The raw data files generated by UPLC–MS/MS were processed using MassLynx software (v4.1) to perform peak integration, calibration, and quantitation for each metabolite. iMAP (http://imap.metaboprofile.cloud/) was used for statistical analyses.

2.10 Statistical analysis

Two α-diversity indices, including abundance-based coverage estimator (ACE) and Chao, were used to analyze the α-diversity. The Bray-Curis distance was adopted to analyze the difference in β-diversity among species composition, which was shown in the PCA diagram. The Wilcoxon rank sum test was employed for both groups for numerical variables not conforming to the normal distribution, and the t test for numerical variables conforming to the normal distribution. The linear discriminant analysis (LDA) effect size (LEfSe) was used to identify the biomarkers with statistical differences between the two groups. QIIME software was adopted to perform core microbiota analysis. Spearman was used to assess the association of GIT microbiota with TC microbiota. $P < 0.05$ indicates a statistically significant difference.

3 Results

3.1 Subjects' clinical characteristics

A total of 39 subjects was recruited in the study, including 20 cases with YGTC and 19 cases with TWTC (Figure 1 and Table 1). The mean age and gender distribution of TC or fecal donors were not statistically different between the two groups (both $P > 0.05$).

Figure 1 Samples of the different TCs
A, TWTC. B, YGTC. Sampling images of TC from the center of the tongue, an area regarded as TC in the traditional tongue diagnosis [4].

3.2 α-Diversity of TC and GIT microbiota in YGTC

The dilution curve of TC and fecal samples tended to be flat or reached the plateau stage, indicating that the sequencing amount of the sample was sufficient and the sequencing depth had covered all species in the sample. Chao and ACE index of TC species in YGTC tended to decrease, but without significant difference ($P > 0.05$). Chao and ACE index of GIT species in YGTC decreased significantly ($P < 0.05$) (Figure 2).

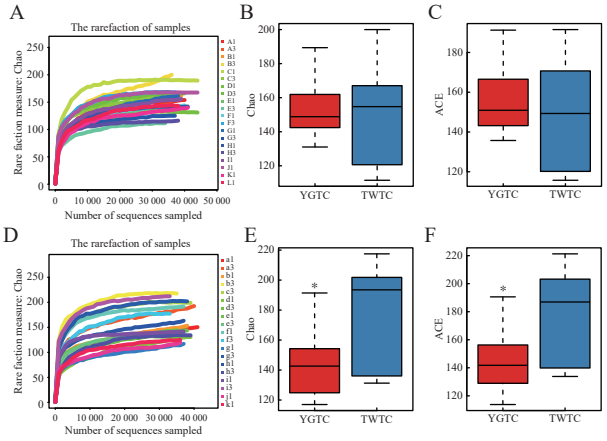

Figure 2 α-Diversity analysis of TC and GIT microbiota
A - C, dilution curve, ACE, and Chao index of TC samples. D - F, dilution curve, ACE, and Chao index of GIT samples. *$P < 0.05$, compared with TWTC.

Table 1 Demographics and clinical characteristics of included subjects

Group	Age (Years)	Gender (M/F)	Chronic gastritis	Gastric/Duodenal ulcer	Fatty liver	Chronic hepatitis	Hepatic cirrhosis	Cholelithiasis
YGTC (n = 20)	48.5 (23-78)	13/7	15	5	8	4	4	3
TWTC (n = 19)	44.5 (25-64)	12/7	0	0	0	0	0	0
P	0.076 6	0.609 4	N/A	N/A	N/A	N/A	N/A	N/A

N/A represents not applicable.

3.3 Information on TC and GIT dominant species

At the genus level, the TC dominant species in two groups included *Prevotella* and *Veillonella*, etc. The GIT dominant species in two groups included *Prevotella* and *Bacteroides*, etc. Although the dominant species in two groups are the same, the relative abundance was different (Figure 3).

3.4 TC and GIT species markers

In the YGTC group, only nine species and their subclasses in TC samples were down-regulated. *Haemophilus*, *Haemophilus Parainfluenzae*, *Pasteurellales,* and *Gammaproteobacteria* contributed the most. A total of 26 species and their subclasses were down-regulated in the GIT, with *Rikenellaceae* contributing the most; six species and their subclasses in the GIT were up-regulated, with *Proteobacteria* contributing the most (Figure 4).

3.5 Spearman correlation analysis on dominant species interaction

Spearman association network of dominant bacteria interaction is to investigate the interaction between different community members, find the interaction mode of co-occurrence or co-exclusion between microbial community members in different habitats, and infer the possible cooperative or competitive relationship between different microorganisms. *Haemophilus* had a negative correlation (competitive relationship) with *Megasphaera*, *Veillonella*, *Actinomyces*, etc. ($P < 0.05$), and a positive correlation (synergistic relationship) with *Fusobacterium*, etc. ($P < 0.05$). *Ruminococcus* was positively correlated with *Roseburia*, *Ascillopsia*, etc. ($P < 0.01$), and negatively correlated with *Neisseria*, etc. ($P < 0.05$; Figure 5). We calculated the Spearman rank correlation coefficient between the dominant genera, whose abundance was located in the top 20, and constructed the associated network for the related advantage where rho > 0.4 and $P < 0.05$.

3.6 Similarity analysis of microbial community structure between TC and GIT

This study conducted principal component analysis (PCA) on the community structure between TC and fecal samples to investigate the similarity between TC and GIT microbial community structure at the genus level. According to Figure 6, it is suggested that there are great differences in the community structure between TC and GIT in the two groups.

3.7 TC and GIT metabolite markers

The detected metabolites mainly included Fumarate reductase, V/A-type ATPase, phosphatidylethanolamine, ascorbate, H_2S, 3-oxo adipate, glycogen/starch, and riboflavin. T1SS were presented in larger amounts in the YGTC. But metagenomic analysis revealed a significant decrease in tryptophan, glycerate-3P, UDP-glucose, and quinone oxidoreductase metabolites in the YGTC subjects.

The inferred metagenomic metabolite markers enriched in YGTC GIT contained inosine monophosphate (IMP), uridine monophosphate (UMP), gamma-aminobutyric acid (GABA), urea, carnosamine, cysteine, methane, acetyl-CoA, and T3SS. While the relative abundance of ribose-5P, histidine, biotin, cobalamin,

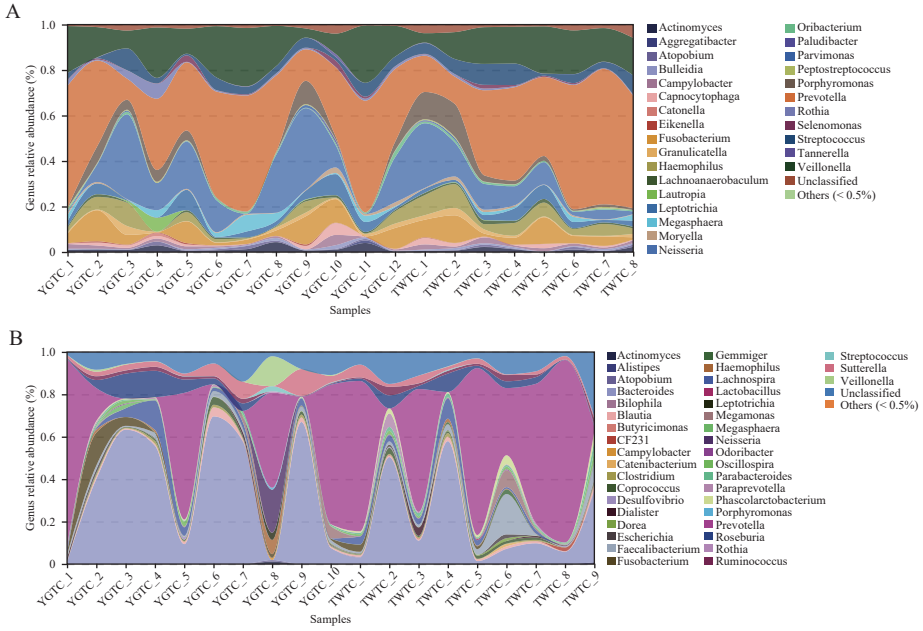

Figure 3 River map of species relative abundance in TC and fecal samples at the genus level

A, TC samples. B, GIT samples.

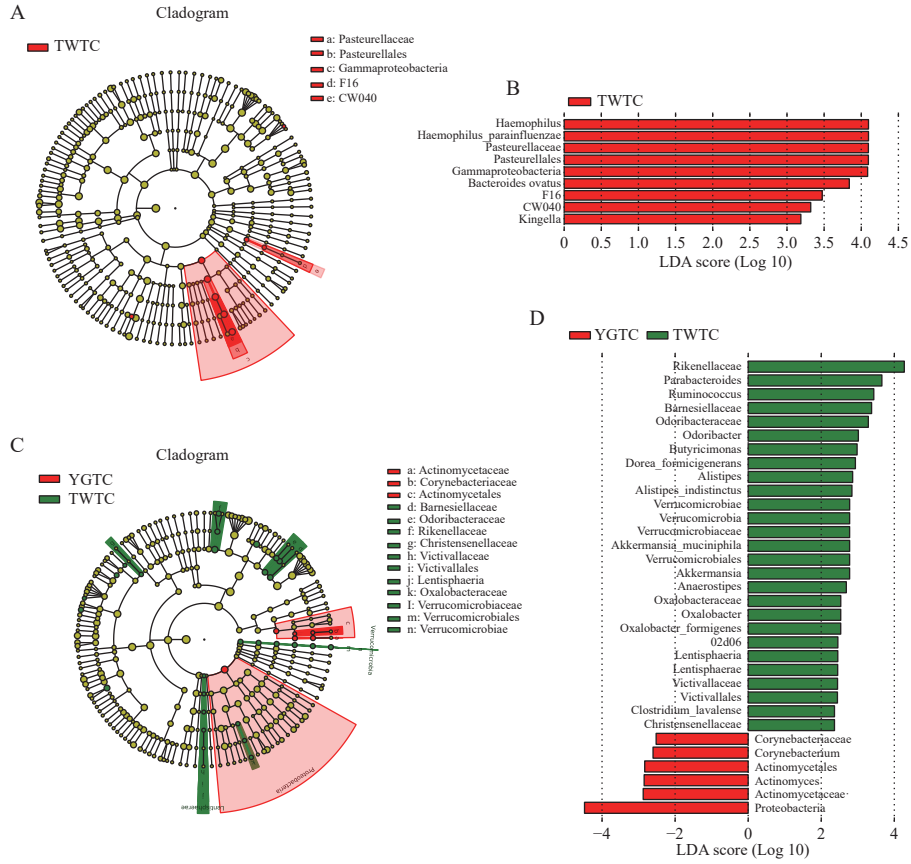

Figure 4 TC and GIT species markers

A, evolutionary branch diagram of TC species. B, histogram of TC LDA score. C, evolutionary branch diagram of GIT species. D, histogram of GIT LDA score. The screening criteria were LDA value > 2.0.

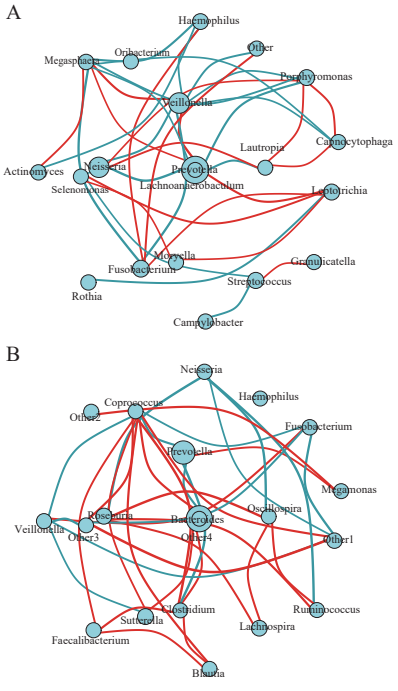

Figure 5 Interaction network of TC and GIT dominant species in YGTC

A, TC. B, GIT. The thickness of the line represents the correlation strength estimated by Spearman correlation analysis, in which a positive correlation is represented by red and a negative correlation by blue.

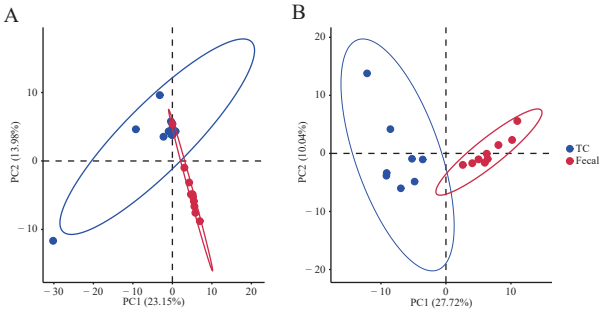

Figure 6 PCA between TC and fecal samples in the YGTC and TWTC

A, YGTC. B, TWTC.

tryptophan, heme, oxaloacetate, blotin, menaquinol, and other metabolites was decreased in YGTC group GIT (Figure 7).

3.8 Differential metabolic pathways in the TC and GIT analyzed by WGS

Figure 8A shows that there were 7 metabolic pathways increased, and 7 metabolic pathways decreased in TC of the YGTC group. Figure 8B shows that there were 11 metabolic pathways up-regulated, and 9 metabolic pathways down-regulated in GIT of the YGTC group.

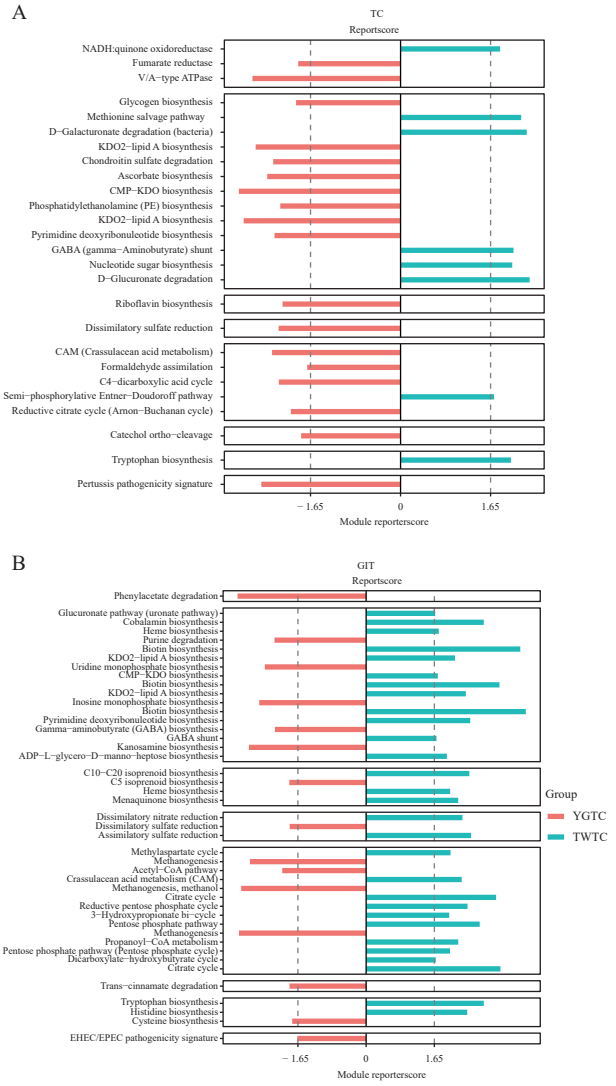

Figure 7 TC and GIT metabolite markers

A, TC metabolite markers. B, GIT metabolite markers. The left and right dotted lines were plus or minus 1.65, and exceeding the dotted lines represented a significant difference.

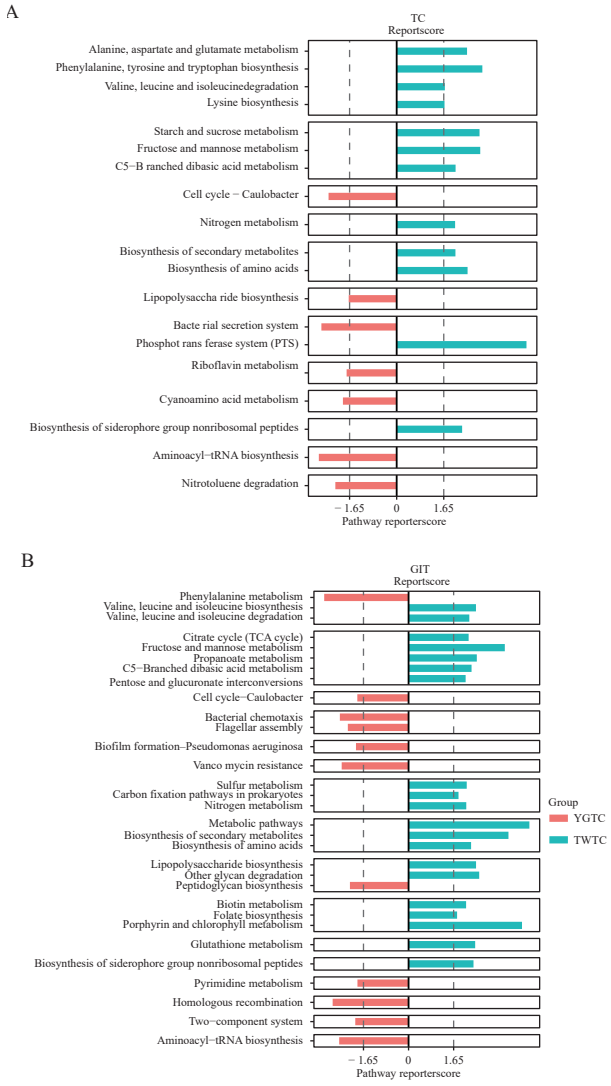

Figure 8 Differential metabolic pathways in the TC and GIT between YGTC and TWTC

A, TC samples. B, GIT samples. The left and right dotted lines were plus or minus 1.65, and exceeding the dotted lines represented significant differences.

4 Discussion

According to the theory of TCM, the tongue image is a mirror for the internal organs, which can reflect the body's physiological and clinicopathological condition. The color, size and form, motion, substances, and coating of the tongue are related to the health state of patients. The disease diagnosis shows that one or more of the diseases were diagnosed in the YGTC subjects, with a focus on two important systems (digestive and endocrine systems), involving several organs such as the liver, gallbladder, gastrointestine, and pancreas, which suggests that the TC was a very sensitive and reliable index that reflected the physiological and pathological status of energy metabolism organs, especially the spleen and stomach in TCM. According to the *Yellow Emperor's Inner Classics* (*Huang Di Nei Jing*, 《黄帝内经》), "the spleen governs transportation and transformation, the spleen transports and transforms food nutrients and water, which are distributed to the whole body and nourishes the four limbs and other parts of the body"; "the spleen and stomach is the acquired base of life and the source of Qi, blood, and body fluid". These opinions approve that the spleen and stomach in TCM are the centers of internal energy circulation.

In our study, significant changes in both GIT microbial richness (by observing Shannon and ACE indexes) and structure (by Bray-Curtis distance matrix) in the YGTC subjects were found when compared with healthy controls. However, no difference was detected in the Shannon and ACE indexes between the YGTC and TWTC groups, which suggests that microbial communities in YGTC did not show significant differences regarding α-diversity and richness, but were hallmarked by a different microbial structure. They mainly resulted from the changed microbial relative abundances [9].

Our research demonstrated that the composition of the GIT microbiome of individuals with the YGTC differed from that of healthy controls, implicating GIT bacteria in the formation mechanism of this disorder. Members of these phyla and genera that were enriched in the GIT microbiota of participants with YGTC were highly heterogeneous, and most of them have been recognized as opportunistic pathogens found to be associated with chronic inflammation and other diseases, such as *Actinomyces* in gut mucosa barrier injury [10], *Corynebacterium* in GIT infection and irritable bowel syndrome [11], and also *Proteobacteria* in diabetes and obesity [12, 13]. The abundance of a diverse set of anti-inflammatory GIT bacteria significantly decreased, especially *Rikenellaceae* [14]. The *Clostridiales*, *Lentisphaerae*, *Oxalobacter formigenes,* and *Verrucomicrobia* [15] with protective effects were also significantly decreased compared with the healthy controls. For example, Oxalate degradation by the probiotic anaerobic bacterium *Oxalobacter formigenes* has high yield and efficiency both in the human colon, which helps to prevent hyperoxaluria and disorders such as the development of kidney stones, serving as a novel approach in reducing the high concentration of foodstuff oxalate content such as tea, coffee, and nuts [16]. Another example of a less familiar gram-negative bacterial species that are associated with healthy individuals but absent or present in very low abundance in individuals with obesity, diabetes, cardiometabolic diseases, and low-grade inflammation is *Akkermansia muciniphila*, which colonizes the GIT mucosal layer and is proposed as a probiotic candidate [17].

The microbial changes in the TC might be the one of formation mechanisms for YGTC. The YGTC showed a strong microbial imbalance when compared with healthy controls, with decreased bacteria abundance including *Gammaproteobacteria* class, *Pasteurellales* order, *Pasteurellaceae* family, *Haemophilus* genus, and *Haemophilus parainfluenzae* species. Moreover, the correlation analysis between TC bacteria revealed that *Megasphaera*, *Veillonella,* and *Actinomyces* genera tended to negatively correlate with the *Haemophilus* genus in YGTC, indicating that *Megasphaera*, *Veillonella,* and *Actinomyces* might also be the main contributor to YGTC. The Human Microbiome Project Consortium found the dominant bacteria presented in the oral cavity was mainly composed of *Haemophilus* and *Actinomyces*, etc., which play a vital role in the maintenance of oral health by contributing to the host defenses preventing exogenous micro-organisms colonization and thus profoundly influencing the host physiology [10, 18]. Whereas an altered relative abundance of oral dominant bacteria, termed dysbiosis, could lead to immune dysregulation and increase a person's risk of developing several diseases [19]. These microbial species, as opportunistic pathogens colonizing the oral cavity, have been reported to be associated with periodontal disease [20, 21], H_2S-producing [22], and other severe and fatal associated microbiota characterization diseases [23].

It was reported that the tongue shares considerable similarities with the gut not only in mucosal epithelia but also in microbial diversity [24]. In contrast, our results indicated TC microbiota showed no substantial difference in β-diversity with the GIT microbiota, and no positive/negative correlation between the TC microbiota and the GIT microbiota was found. The underlying reasons for this are not clear but may be related to differences in the site-specific conditions. The ecological niches vary according to mucosal architecture, local host immune response, and environmental exposure (i.e., temperature, humidity, and nutrient and oxygen availability), hence affecting bacterial community structure [25]. However, despite being highly independent in microbiota structure, our evidence suggested that GIT and TC share similar metabolic pathways. Phenotypic predictions detected a high abundance of potentially pathogenic on samples both fecal and TC in YGTC subjects, such as *Actinobacillus*, *Haemophilus*, and *Proteobacteria*. Both GIT and TC in YGTC subjects were characterized by several pathogenic pathways and seemed to have important functions in cell motility (flagellar assembly, bacterial chemotaxis), increased virulence, biofilm formation, stress resistance, antibiotic resistance, and pathogenicity. The YGTC subjects were supposed to be much more susceptible to risks, including inflammatory disease, than healthy controls. Metabolic pathway analysis indicated that both TC and GIT metabolic pathways associated with energy metabolisms, such as carbohydrate metabolism, glycan biosynthesis and metabolism, metabolism of cofactors and vitamins, glutathione metabolism, valine, leucine, and isoleucine biosynthesis and degradation, were down-regulated in YGTC subjects compared with the healthy controls. This means that the tongue-gut axis was a two-way pathway, which connected and worked through microbial metabolic pathways and molecules, to jointly monitor the health or disease state of the host.

The differential metabolites in TC, which reflected early changes in disease, could also supply the fecal metabolite markers [26]. The metabolite markers identified to be significantly up-/down-regulated in the YGTC, such as fumarate reductase, quinone oxidoreductase, V/A-type ATPase, phosphatidylethanolamine, ascorbate, H_2S, 3-oxo adipate, glycogen/starch, riboflavin, and T1SS, were involved in several key oxidative metabolic pathways including glycolysis pathway (fumarate reductase [27]), redox regulation (riboflavin and ascorbate), energy metabolism (quinone oxidoreductase [28]), and transport (V/A-type ATPase [29]). The observed latent GIT metabolite markers in YGTC subjects were found to be associated with amino acid metabolism (cysteine and GABA), carbohydrate and SCFA metabolism (acetyl-CoA and oxaloacetate [30]), nucleotide metabolism (IMP and

UMP [31, 32]), metabolism of cofactors and vitamins (biotin, heme, and cobalamin), pathogenicity, toxins, and the biosynthesis of other secondary metabolites.

However, there are still some limitations to our research. First, the sample size for this study is comparatively small, so these findings should be validated using a larger number of subjects and other cohorts. Next, the TC is often temporary, and the association of YGTC with the disease should be verified. Besides, some of the microbiota and metabolic differences may be related to differences in disease rather than TC status. Therefore, futher investigation is warranted to delineate microbiota and metabolic changes due to disease diagnosis and TC.

5 Conclusion

Tongue image diagnosis can be an effective, noninvasive, and inexpressive method to perform an auxiliary diagnosis anywhere. However, the recognition of the use of tongue images by TCM doctors is subjective and challenging. We found that microbial intestinal dysbiosis presented in YGTC subjects, which is a result of the decrease in richness and changes in the global structure of the GIT microbiota. Therefore, this study provides strong scientific support for the theory of tongue image diagnosis in TCM. TC diagnosis could be used as an early detection or primary screening method for spleen and stomach diseases in TCM. Moreover, YGTC images could provide early warning for potential infectious diseases, digestive system diseases, and endocrine and metabolic diseases *in vivo*.

Fundings

China Central Finance Improvement Project for the National Key Laboratory of Traditional Chinese Medicine (China Central Finance CS [2021] No. 151), the Special Key Project of Strengthening Science and Technology of Guangdong Province with Traditional Chinese Medicine (20215002), and Shenzhen Basic Research Discipline Layout Project (JCYJ20170412161254416).

Competing interests

The authors declare no conflict of interest.

References

[1] VAN GL, SLOT D, VAN DSE, et al. Tongue coating in relationship to gender, plaque, gingivitis and tongue cleaning behaviour in systemically healthy young adults. International Journal of Dental Hygiene, 2020, 18(1): 62–72.

[2] YE J, CAI X, CAO P. Problems and prospects of current studies on the microecology of tongue coating. Chinese Medicine, 2014, 9(1): 9–12.

[3] LIANG X, WANG Q, JIANG Z, et al. Clinical research linking traditional Chinese medicine constitution types with diseases: a literature review of 1639 observational studies. Journal of Traditional Chinese Medicine, 2020, 40(4): 690–702.

[4] SUN ZM, ZHAO J, QIAN P, et al. Metabolic markers and microecological characteristics of tongue coating in patients with chronic gastritis. BMC Complementary and Alternative Medicine, 2013, 13: 227–236.

[5] HSU PC, WU HK, HUANG YC, et al. The tongue features associated with type 2 diabetes mellitus. Medicine (Baltimore), 2019, 98(19): e15567–e15572.

[6] HU J, HAN S, CHEN Y, et al. Variations of tongue coating microbiota in patients with gastric cancer. Biomed Research International, 2015: 173729–173735.

[7] ZHAO Y, MAO YF, TANG YS, et al. Altered oral microbiota in chronic hepatitis B patients with different tongue coatings. World Journal of Gastroenterol, 2018, 24(30): 3448–3461.

[8] LI CD, FANG CY. Diagnostics of Traditional Chinese Medicine. Beijing: China Press of Traditional Chinese Medicine, 2021: 48-50.

[9] DU Q, FU M, ZHOU Y, et al. Sucrose promotes caries progression by disrupting the microecological balance in oral biofilms: an *in vitro* study. Scientific Reports, 2020, 10(1): 2961–2972.

[10] LI J, LI Y, ZHOU Y, et al. Actinomyces and alimentary tract diseases: a review of its biological functions and pathology. Biomed Research International, 2018, 2018: 3820215.

[11] XIAO L, LIU Q, LUO M, et al. Gut microbiota-derived metabolites in irritable bowel syndrome. Frontiers in Cellular and Infection Microbiology, 2021, 11: 729346–729356.

[12] LIU F, LIU A, LU X, et al. Dysbiosis signatures of the microbial profile in tissue from bladder cancer. Cancer Medicine, 2019, 8(16): 6904–6914.

[13] HU B, DONG Y, ZHOU W, et al. Effect of *Inonotus obliquus* polysaccharide on composition of the intestinal flora in mice with acute endometritis. PLoS One, 2021, 16(11): e259570–e259580.

[14] TAO JH, DUAN JA, JIANG S, et al. Polysaccharides from *Chrysanthemum morifolium* Ramat ameliorate colitis rats by modulating the intestinal microbiota community. Oncotarget, 2017, 8(46): 80790–80803.

[15] CHOU YT, LIU TT, YANG UC, et al. Intestinal SIRT1 deficiency-related intestinal inflammation and dysbiosis aggravate TNFα-mediated renal dysfunction in cirrhotic ascitic mice. International Journal of Molecular Sciences, 2021, 22(3): 1233–1251.

[16] KARAMAD D, KHOSRAVI-DARANI K, HOSSEINI H, et al. Evaluation of Oxalobacter formigenes DSM 4420 biodegradation activity for high oxalate media content: an *in vitro* model. Biocatal Agric Biotechnol, 2019, 22: 101378–101401.

[17] MACCHIONE IG, LOPETUSO LR, IANIRO G, et al. Akkermansia muciniphila: key player in metabolic and gastrointestinal disorders. European Review for Medical and Pharmacological Sciences, 2019, 23(18): 8075–8083.

[18] GAONKAR PP, PATANKAR SR, TRIPATHI N, et al. Oral bacterial flora and oral cancer: the possible link. Journal of Oral & Maxillofacial Pathology, 2018, 22(2): 234–238.

[19] ZHU XX, YANG XJ, CHAO YL, et al. The potential effect of oral microbiota in the prediction of mucositis during radiotherapy for nasopharyngeal carcinoma. EBioMedicine, 2017, 18: 23–31.

[20] SHARMA N, BHATIA S, SODHI AS, et al. Oral microbiome and health. AIMS Microbiology, 2018, 4(1): 42–66.

[21] MOGILNICKA I, BOGUCKI P, UFNAL M. Microbiota and malodor-etiology and management. International Journal of Molecular Sciences, 2020, 21(8): 2886–2906.

[22] QING Y, XU L, CUI G, et al. Salivary microbiome profiling reveals a dysbiotic schizophrenia-associated microbiota. NPJ

Schizophrenia, 2021, 7(1): 51–60.
[23] HERNANDEZ-TERAN A, MEJIA-NEPOMUCENO F, HERRERA MT, et al. Dysbiosis and structural disruption of the respiratory microbiota in COVID-19 patients with severe and fatal outcomes. Scientific Reports, 2021, 11(1): 21297–21309.
[24] BIK EM, ECKBURG PB, GILL SR, et al. Molecular analysis of the bacterial microbiota in the human stomach. Proceedings of the National Academy of Sciences of the United States of America, 2006, 103(3): 732–737.
[25] DE SPW, BOGAERT D. Unraveling the molecular mechanisms underlying the nasopharyngeal bacterial community structure. mBio, 2016, 7(1): e9–e16.
[26] YUAN L, YANG L, ZHANG S, et al. Development of a tongue image-based machine learning tool for the diagnosis of gastric cancer: a prospective multicentre clinical cohort study. eClinicalMedicine, 2023, 57: 101834.
[27] MESSNER KR, IMLAY JA. Mechanism of superoxide and hydrogen peroxide formation by fumarate reductase, succinate dehydrogenase, and aspartate oxidase. Journal of Biological Chemistry, 2002, 277(45): 42563–42571.
[28] OHNISHI T, OHNISHI ST, SALERNO JC. Five decades of research on mitochondrial NADH-quinone oxidoreductase (complex I). Biological Chemistry, 2018, 399(11): 1249–1264.
[29] KHOLGHI M, TOORCHI M, BANDEHAGH A, et al. Comparative proteomic analysis of salt-responsive proteins in canola roots by 2-DE and MALDI-TOF MS. Biochimica et Biophysica Acta Proteins and Proteomics, 2019, 1867(3): 227–236.
[30] RAETHONG N, NAKPHAICHIT M, SURATANNON N, et al. Analysis of human gut microbiome: taxonomy and metabolic functions in Thai adults. Genes, 2021, 12(3): 331–342.
[31] JIN M, YANG F, YANG I, et al. Uric acid, hyperuricemia and vascular diseases. Frontiers in Bioscience, 2012, 17: 656–669.
[32] FREDERICK A, SHERER K, NGUYEN L, et al. Triacetyluridine treats epileptic encephalopathy from CAD mutations: a case report and review. Annals of Clinical and Translational Neurology, 2021, 8(1): 284–287.

黄腻苔人群舌苔与肠道菌群微生态特征及其相关性研究

刘展艳[a, b†], 李芷悦[b†], 朱关保[b, c], 刘雅倩[b], 彭清华[a*], 吴正治[b, d*]

a. 湖南中医药大学中医学院, 湖南 长沙 410208, 中国
b. 深圳大学第一附属医院深圳市老年医学研究所, 广东 深圳 518035, 中国
c. 广西中医药大学研究生院, 广西 南宁 530200, 中国
d. 宁波卫生职业技术学院吴正治院士工作站, 浙江 宁波 315800, 中国

【摘要】目的 研究黄腻苔人群的舌苔和肠道微生物菌群结构和代谢特征，探讨黄腻苔人群舌苔和肠道菌群代表性的代谢标志物和代谢通路。**方法** 于 2021 年 12 月 1 日至 2022 年 10 月 30 日采集黄腻苔及薄白苔受试者的舌苔及大便样本。16S rRNA 及宏基因组测序技术对 2 组受试者的舌苔和粪便样本进行菌群鉴定；并对 2 组样品进行菌群 α-多样性分析、主成分分析（PCA）和 Spearman 相关性分析；超高效液相色谱联用串联质谱（UPLC-MS/MS）进行代谢组学分析及代谢通路富集分析。**结果** 本研究共招募 20 例黄腻苔受试者和 19 例薄白苔受试者。在菌群属水平，2 组受试者的舌苔菌群及肠道菌群的优势菌种大致相同，但是相对峰度差异明显，黄腻苔受试者舌苔及粪便样本中潜在致病菌丰度较高。黄腻苔受试者的舌苔样品中有 9 种微生物下调，粪便样品中有 26 种微生物下调，6 种微生物上调。α-多样性分析显示，黄腻舌苔受试者舌苔菌群的 Chao 和 ACE 指数有下降趋势，但差异无统计学意义（$P > 0.05$）；粪便样本菌群的 α-多样性明显降低，Chao 和 ACE 指数显著下降（$P < 0.05$）。主成分分析结果显示，2 组受试者的舌苔和粪便样本的菌群结构差异较大。Spearman 相关性分析，同一受试者舌苔和粪便微生物在菌种在门和属水平上无相关性（$P > 0.05$）。代谢组学结果显示黄腻苔的舌苔样本中富马酸还原酶、V/A 型 ATP 酶、磷脂酰乙醇胺等含量增加，甘油酸-3P，UDP-葡萄糖和醌氧化还原酶代谢物等代谢物含量减少；大便样本中单磷酸肌苷（IMP）、单磷酸尿苷（UMP）、γ 氨基丁酸等含量增加，核糖-5P、组氨酸、生物素、钴胺素等含量减少。代谢通路分析显示黄腻苔的舌苔样本及粪便样本在包括氨基酸代谢、碳水化合物代谢、氮代谢及能量代谢等多种代谢通路相对丰度较低。**结论** 舌苔和肠道微生物群或代谢物的结构和功能的变化可能是黄腻苔形成的潜在生物学基础。

【关键词】 肠道菌群；黄腻苔；微观辨证；16S rRNA；宏基因；代谢组学